PHOTOELECTRONICS

UDC 621 PACS: 81.05.-t
EDN: GYTPJU

Defects formation in SiO_2 layer during diffusion processes in silicon

© K. O. Boltar[1,2], M. N. Vildyaeva[1], N. A. Irodov[1], E. A. Klimanov[1,3,*], A. V. Lyalikov[1], V. A. Malygin[1], D. S. Molchanov[1], E. A. Makarova[1]

[1] RD&P Center ORION, JSC, Moscow, 111538 Russia
[*] E-mail: klimanov3@mail.ru
[2] Moscow Institute of Physics and Technology (National Research University), Moscow Region, Dolgoprudny, 141701 Russia
[3] MIREA – Russian Technological University (RTU MIREA), Moscow, 119454 Russia

Received 13.12.2024; revised 13.03.2025; accepted 07.04.2025
Scientific specialty code: 1.3.11

The influence of diffusion of phosphorus from a liquid source (POCl3) and a solid source (aluminum metaphosphate (AMP)) on the formation of local defects in SiO_2 layers on the silicon surface has been analyzed. The probable cause of defects formation has been established to be local melt-through of the oxide layer by liquid phosphorus-silicate glass due to a silicon-rich solid phase formation. The defect depth is proportional to its diameter and decreases as the process temperature drops.

Keywords: defect, diffusion, silicon.

DOI: 10.51368/1996-0948-2025-2-39-45

1. Introduction

The cycle of manufacturing silicon photodiodes typically involves the diffusion of high concentrations of boron and phosphorus to form doped regions and p–n junctions. The process of phosphorus diffusion often leads to the formation of local defects in the dielectric layers acting as a protective mask [1–4]. The said defects can give rise to the local n^+ channels in p^+–n junctions, thus causing leakage currents therein, as well as defects in MOS-IC and CCD structures.

The goal of this paper is to study the formation patterns of these defects in order to determine the conditions reducing their influence on leakage currents of p^+–n junctions.

2. Experiment

To determine the defect parameters (morphology, size and concentration), samples with p^+–n junctions sized 1.4×1.4 mm^2 were made using wafers of monocrystalline silicon (Cz-Si) of n-type with a diameter of 100 mm, a specific resistance of 4–5 Ω·cm and orientation (100).

The manufacturing cycle included the oxidation in H_2O+HCl, vapor,

photolithography, predeposition (deposition) of boron from boron nitride BN wafers at a temperature of 1000 °C, boron diffusion (drive-in), predeposition (deposition) of phosphorus from a liquid source ($POCl_3$) and solid source wafers (aluminum metaphosphate (AMP) at temperatures of 900–1050 °C. The duration of phosphorus predeposition at different temperatures was selected within the range of 10–40 minutes in order to ensure the same thickness of the phosphorsilicate glass (PSG).

The concentration and distribution of local defects over the plate were determined on the manufactured samples using an optical microscope. A scanning electron microscope, an atomic force microscope and a profilometer were used to determine the size and shape of defects. The constituent elements of defects were determined by X-ray spectroscopy.

3. Results

Major results are summarized below.

1. Most oxide defects that can be observed are pits of round shape with a diameter of 2 to 40 μm, with the depth proportional to their diameter (Fig. 1). When the defect depth reached the value equal to the SiO_2 thickness, through holes could be seen (in an oxide of 0.4 μm in thickness with a pit diameter more than 10 μm). The distributions of defects by diameter and depth are correlated with each other and are shown in Fig. 2.

2. The defect surface profile depends on its depth and diameter. Smooth walls can be observed on the surface profile of the defect with a depth of 0.15–0.2 μm. If the defect depth increases and approach to the dielectric thickness, a rough profile can be observed (Fig. 3).

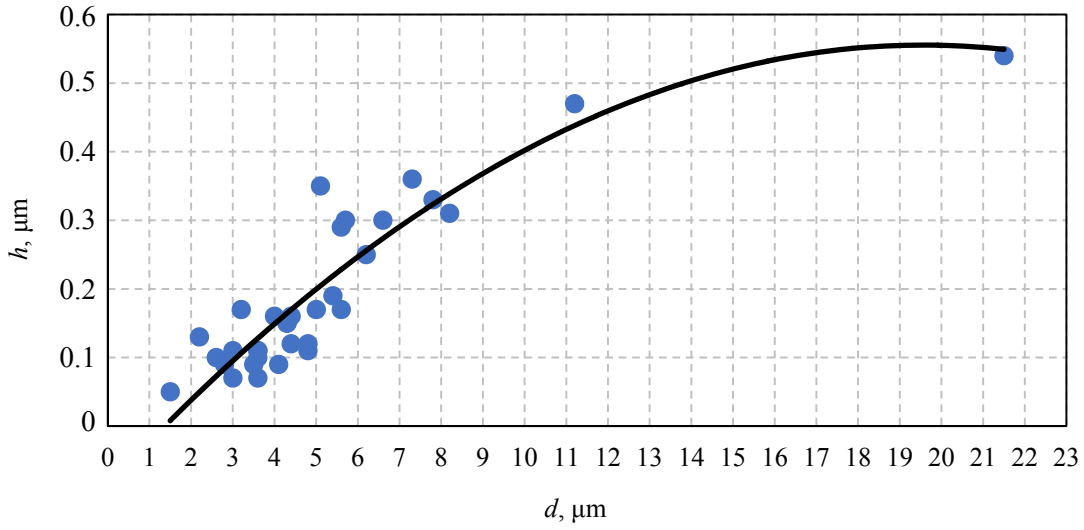

Fig. 1. Defect depth vs defect diameter

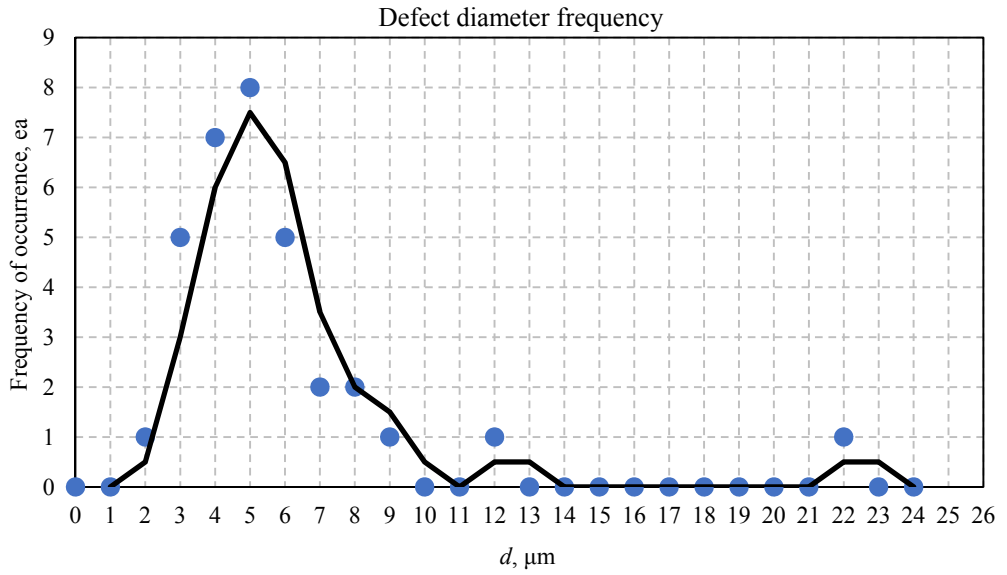

a)

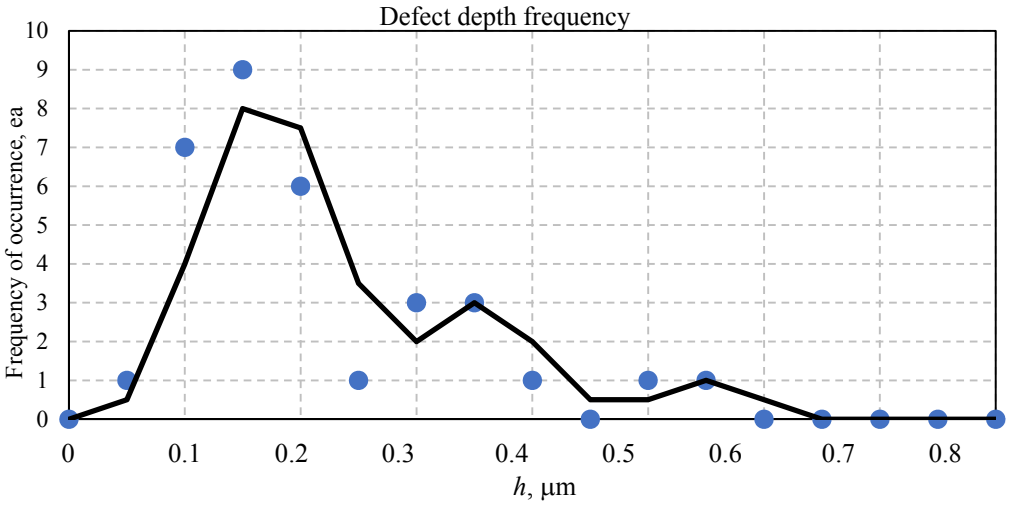

b)

Fig. 2. Frequency of defect occurrence vs. diameter and depth

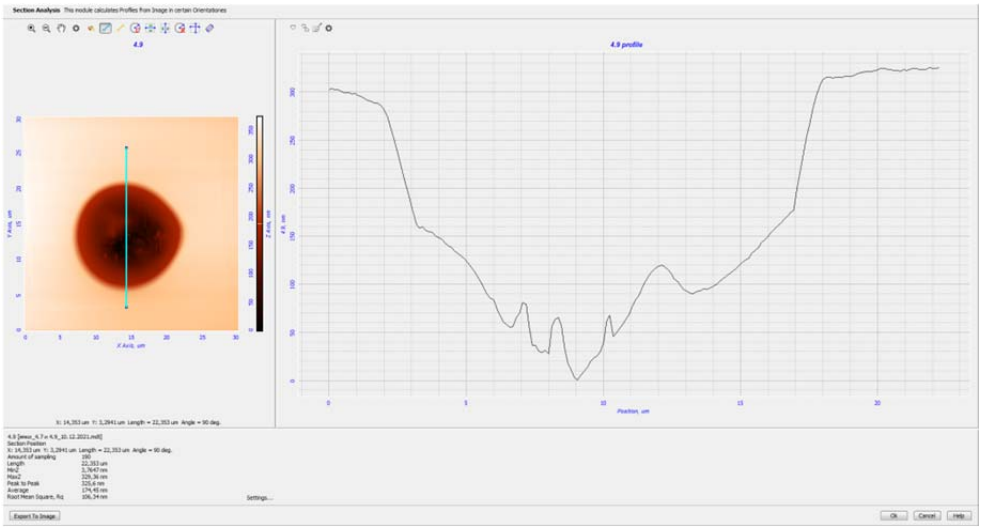

Fig. 3. Defect surface profil

In the center, the defect is often shaped as a rosette (Fig. 4). The atomic fraction of silicon in the defect reaches 65–68% (in SiO_2 – 47 %), the atomic fraction of oxygen is 19–35 % (in SiO_2 – 53 %), and that of phosphorus is 0.7 %. The accuracy of determining the concentration of elements ranged from 5 to 20 % of the given values for different elements and samples (Table 1).

3. The distribution of defects over the plate area is random, regardless of the source of diffusant ($POCl_3$ or AMP) used and layout of plates in the reactor: vertical or horizontal relative to the gas flow.

4. The density of defects depends on the quality and thickness of the protective dielectric film: the film of the same sample is thinner over a thicker (field) oxide formed in the *n*-region than over an oxide grown in the p^+-region pre-doped as a result of boron diffusion. Boron diffusion did not result in the formation of defects in the field oxide. Decrease of the phosphorus concentration (increase of surface resistance Rs) leads to decrease of the defects density (for example, when the process temperature drops) (Table. 2).

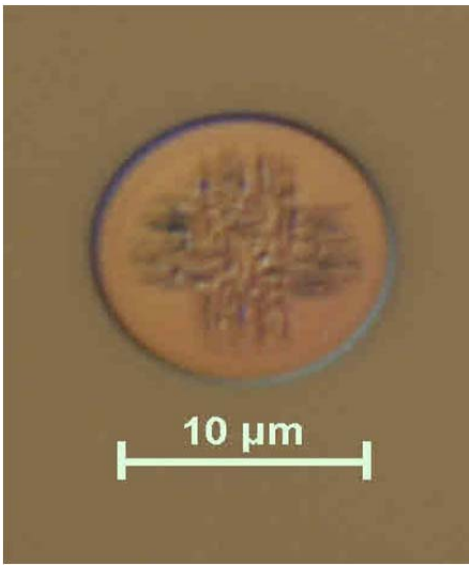

Fig. 4. Optical view of the "rosette" defect in the central area

Table 1

Content of elements in the solid phase (Net Int. – Total intensity of the peak corresponding to the element, minus the background)

Element	Weight %	Atomic %	Net Int.	Error %
C K	5.8	11.6	15.1	12.0
O K	13.1	19.5	197.2	10.5
Si K	80.2	68.2	15980.8	4.5
P K	0.9	0.7	39.4	11.3

Table 2

Defect density vs. surface resistance (Rs) and diffusion temperature

Temperature, °C	900	970	1000	1050
Defect density $D < 10$ μm, mm^{-2}	8.1	13.8	13.0	46.6
Defect density D= 10-40 μm, mm^{-2}	2.0	2.5	3.0	8.9
Defect density $D>40$ μm, mm^{-2}	0.4	0.5	0.7	0.7
Average value of surface resistance, Rs, Ω/□	157.4	24.5	12.4	4.5
Diffusant source	$POCl_3$	$POCl_3$	AMP	$POCl_3$

5. Heat treatment in the reactor in the absence of a diffusant does not lead to defects. Consequently, formation of defects has nothing to do with particles entering the samples from the reactor walls or from the carrier gas flow (N_2, O_2).

4. Discussion

Mechanism of microdefect formation [7] can be local melt-through of the oxide layer by liquid phosphorus-silicate glass (PSG) at the diffusion temperature. When the PSG layer solidifies during cooling of the samples, local areas with the increased concentration of phosphorus (P_2O_5) may form, their solidification temperature being lower than in the rest of the PSG layer. Such liquid drop dissolves phosphorus and other impurities when cooled, which further reduces its solidification temperature. Liquid phase regions that diffuse into the SiO_2 layer are formed, which results in pits of various depths determined by the defect radius (liquid phase amount) (see Fig. 1). When the pit depth exceeds the oxide thickness, the liquid glass interacts with silicon to form a silicon- and phosphorus-rich crystalline phase at the pit bottom (see Fig. 3, 4 and Table 1).

Formation of the crystalline phase while a through defect is developing may be related to the devitrification of amorphous SiO_2 under the influence of liquid phosphorsilicate glass acting as a mineralizer, with the silicon-rich phase formed. Local melting of the oxide can be accelerated by defective areas formed in it during growth [1].

As can be seen on the curve in Fig. 1, defects larger than 10 μm in diameter have a depth more than 0.4 μm, which results in a through hole in the oxide of the specified thickness and interaction with silicon to form n^+-channels and a rosette-shaped solid phase. Smaller defects do not reach the silicon surface and cannot be a reason for impaired current-voltage characteristics. The curve shows that the more the oxide thickness, the weaker the influence of larger diameter defects on the current-voltage characteristics is. Thus, when the oxide thickness is 0.6 μm, defects with a diameter of about 20 μm are not through.

Maxima occurring in the size distributions of pit diameters and depths (see Fig. 2) may be caused by the curve of the density of liquid phase nucleation centers vs. substrate temperature, which has a maximum at a certain value of liquid vapor supersaturation [5, 6]. Since the diffusion

process was completed by slow cooling of the samples in the furnace, there is a temperature range where the maximum number of centers form. The radius of the arising particles of the new phase is determined by the supersaturation value [5]:

$$R = \frac{2\sigma v}{RT \ln \frac{p}{p_0}},$$

where σ is surface tension at the liquid-vapor interface, v is molar volume of the liquid, ln p/p_0 is supersaturation value, p, p_0 are vapor pressure over the drop and equilibrium pressure value.

Since decrease in the phosphorus concentration in PSG should reduce the probability of local areas with the increased concentration of P_2O_5, decrease of the surface resistance as the diffusion temperature grows leads to the increase of defect diameter (see Table 2) and depth, thus impairing the current-voltage characteristics of the *p–n* junctions. It should be considered that the surface resistance shall not exceed 150 Ω/□ to ensure low contact resistance.

Conclusions

1. The influence of diffusion of phosphorus from a liquid source (POCl3) and a solid source (aluminum metaphosphate (AMP)) on the formation of local defects in SiO_2 layers and on the silicon surface has been analyzed.

2. The probable cause of defect formation has been established to be local melt-through of the oxide layer by liquid phosphorus-silicate glass due to a silicon-rich solid phase formed.

3. The defect depth is proportional to its diameter and decreases as the process temperature drops and the oxide thickness increases, which reduces the probability of n^+ channels in silicon.

4. The defect density is higher on the oxide built up on the boron-doped p^+-regions.

REFERENCES

1. Blackstone S., Henry W., Jastrzebski L. and Fisher A. W., Journal of Electrochemical Society **3**, 667–668 (1982).

2. Storch W., Mohr U., Elstner L. and Leihkauf R., Phys. Stat. sol.(a) **132**, K109 (1992).

3. Miyashita M., Fukui H., Kubota A., Samata S., Hiratsuca H. and Matsushita Y. International Conference on Solid State Devices and Materials. Yocohama, 1991, pp. 568–570.

4. Pani S. K., Hogan R. H., Pandurangan M., Zhang J. and Koesan P., J. Vac. Sci. Technol. B **35** (6), 061206-1/5 (2017).

5. Tairov Yu. M. and Tsvetkov V. F. Texnologiya poluprovodnikovy`x i die`lektricheskix materialov, Moscow, Vy`sshaya shkola, 1983.

6. Fizicheskaya ximiya silikatov / Ed. Pashhenko A. A., Moscow, Vy`sshaya shkola, 1986.

7. Vil'dyaeva M. N., Makarova E. A., Klimanov E. A., Lyalikov A. V. and Malygin V. A., Applied Physics, № 5, 53 (2021).

8. Bare G., Madar R. and Bernard C., Journal of Electrochemical Society **138** (9), 2830–2835 (1991).

About authors

Konstantin Olegovich Boltar, Head of Scientific and Technical Complex, Doctor of Physics and Mathematics, RD&P Center ORION, JSC (111538, Russia, Moscow, Kosinskaya Ulitsa, 9). Moscow Institute of Physics and Technology (National Research University) (141701, Russia, Moscow Region, Dolgoprudny, Institutsky Per., 9). E-mail: boltarko@yandex.ru SPIN code 9249-2720, Author ID 171355

Maria Nikolaevna Vildyaeva, Engineer Cat. 1, RD&P Center ORION, JSC (111538, Russia, Moscow, Kosinskaya Ulitsa, 9). E-mail: mari.vildyaeva@mail.ru

Nikita Alexandrovich Irodov, Head of the Area, RD&P Center ORION, JSC (111538, Russia, Moscow, Kosinskaya Ulitsa, 9). E-mail: irodov.mephi@yandex.ru SPIN code 8864-8834, Author ID 777457

Evgeniy Alekseevich Klimanov, Senior Research Assistant, Professor, Doctor of Technical Sciences, RD&P Center ORION, JSC (111538, Russia, Moscow, Kosinskaya Ulitsa, 9). MIREA – Russian Technological University (RTU MIREA) (119454, Russia, Moscow, Prospekt Vernadskogo, 78). E-mail: klimanov3@mail.ru SPIN code 7697-4688, Author ID 171375

Alexey Vladimirovich Lyalikov, Leading Engineer, RD&P Center ORION, JSC (111538, Russia, Moscow, Kosinskaya Ulitsa, 9).

Vladislav Anatolievich Malygin, Engineer, RD&P Center ORION, JSC (111538, Russia, Moscow, Kosinskaya Ulitsa, 9). E-mail: mva1431@yandex.ru SPIN code 9416-8272, Author ID 1240051

Dmitry Sergeevich Molchanov, Engineer, RD&P Center ORION, JSC (111538, Russia, Moscow, Kosinskaya Ulitsa, 9).

Elina Alekseevna Makarova, Engineer Cat. 2, RD&P Center ORION, JSC (111538, Russia, Moscow, Kosinskaya Ulitsa, 9).